Short-term modifications in the chemical structure of wood charcoals: Implications for anthracological investigations

Frédéric Delarue, Amir Ghavidel, Katell Quénéa, Ludovic Bellot-Gurlet, Eva Rocha, S. Coubray, François Baudin, David Sebag, Michel Lemoine, Emmanuel Aubry, et al.

Journal of Archaeological Science: Reports 57 (2024) 104672

Contents lists available at ScienceDirect

Journal of Archaeological Science: Reports

journal homepage: www.elsevier.com/locate/jasrep

Short-term modifications in the chemical structure of wood charcoals: Implications for anthracological investigations

Frédéric Delarue [a,*,1], Amir Ghavidel [a,b,1], Katell Quénéa [a], Ludovic Bellot-Gurlet [c], Eva Rocha [a,b], Sylvie Coubray [b], François Baudin [d], David Sebag [e], Michel Lemoine [b], Emmanuel Aubry [a], Florence Savignac [d], Alexa Dufraisse [b]

[a] CNRS, EPHE, PSL, UMR 7619 METIS, Sorbonne Université, 4 Place Jussieu 75005, Paris Cedex 05, France
[b] UMR 7209 - AASPE-CNRS/MNHN, Archéozoologie, Archéobotanique : Sociétés, Pratiques et Environnements, CP56, 55 rue Buffon 75005, Paris, France
[c] MONARIS UMR8233, Sorbonne Université, CNRS, 4 Place Jussieu 75005, Paris, France
[d] Sorbonne Université - CNRS, Institut des Sciences de la Terre de Paris, UMR ISTeP 7193, 75005, Paris, France
[e] IFP Energies Nouvelles, Earth Sciences and Environmental Technologies Division, 1 et 4 Avenue de Bois-Préau 92852, Rueil-Malmaison, France

ARTICLE INFO

Keyword:
^{13}C stable isotope composition
Fourier-Transform Infrared spectroscopy
Raman spectroscopy
Rock-Eval® thermal analysis
Wood charcoal

ABSTRACT

Archaeological wood charcoals offer a unique window to study paleoclimates through their ^{13}C isotope composition ($\delta^{13}C$) provided that (i) past heating temperatures are assessed to correct $\delta^{13}C$ modifications related to carbonisation, and (ii) they have not been modified by post-depositional processes occurring in soil after their formation. Our goal was to assess how post-depositional processes can modify (i) the determination of past heating temperatures by Raman thermometry and (ii) the $\delta^{13}C$ signature of charcoals, notably through the occurrence of exogenous organic matter (OM). To this end, short-term post-depositional processes were simulated on oak and pine charcoals – produced at 400 and 600 °C – incubated in vermicompost for 6 months. While almost all the studied charcoals showed no evidence of the occurrence of exogenous OM, pine charcoal produced at 400 °C appeared to be subjected to an organic coating with incubation time. This organic coating may have led to a decrease in the H_D/H_G ratio, a proxy of carbonisation temperatures obtained from Raman spectra. In contrast, the H_D/H_G ratio increased in oak charcoal produced at 400 and 600 °C at certain incubation times. Although the processes behind these modifications remain unclear, this investigation highlights that the Raman thermometer may be biased when assessing the heating temperatures of archaeological charcoals. In addition, subtle modifications in the chemistry of pine charcoal produced at 400 °C were enough to yield an increase in $\delta^{13}C$ by up to 0.3 ‰ at the short-term scale of our incubation experiments. This study suggests that long-term experiments are necessary to assess the effect of post-depositional processes on the chemical structure of charcoals and to provide a valuable framework to minimize potential biases in the use of Raman thermometry and of the $\delta^{13}C$ signature.

1. Introduction

Charcoals, which are by-products of the pyrolysis of plant biomass, can persist in soils and sediments for centuries to millennia (Schmidt and Noack, 2000; Sigmund et al., 2021). Charcoals are ubiquitous artifacts from archaeological settings testifying to complex interactions between past societies and their environment (Marguerie and Hunot, 2007; Salavert and Dufraisse, 2014). In addition, archaeological charcoals may also contain information about paleoclimate changes, notably according to their stable ^{13}C isotope composition ($\delta^{13}C$; Ferrio et al., 2006; Hall et al., 2008; Aguilera et al., 2009; Masi et al., 2013; Caracuta et al., 2016; Baton et al., 2017; Audiard et al., 2021) since the $\delta^{13}C$ of the original woods is a function of the combined effects of environmental variables – precipitation, humidity and evapotranspiration – affecting water availability (Fiorentino et al., 2015; Bonal et al., 2017).

In addition to these effects, the $\delta^{13}C$ of archaeological charcoals also varies as a function of the effects of (i) the degree of carbonisation and of (ii) post-depositional processes including modifications of $\delta^{13}C$ by

* Corresponding author at: UMR 7619 METIS, 4 place Jussieu, Tour 46/56, 3ème étage 75252, Paris Cedex.
E-mail address: frederic.delarue@upmc.fr (F. Delarue).
[1] these authors contributed equally to this manuscript.

https://doi.org/10.1016/j.jasrep.2024.104672
Received 15 October 2023; Received in revised form 18 June 2024; Accepted 1 July 2024

inorganic phases (e.g. carbonates) and exogenous organic matter (OM).

Numerous studies have shown that carbonisation leads to (i) the degradation of cellulose and hemicellulose and (ii) an enhanced degree of aromaticity. As cellulose and hemicellulose are relatively enriched in ^{13}C, a progressive decline in $\delta^{13}C$ values is classically observed during carbonisation (Turney et al., 2006; Ascough et al., 2008; Mouraux et al., 2022). By correcting the effect of carbonisation on $\delta^{13}C$ as a function of heating temperatures or by comparing charcoals having been subjected to similar heating temperatures, several authors have used the $\delta^{13}C$ variations to reconstruct past climate with charred woods (Ferrio et al., 2006; Hall et al., 2008; Aguilera et al., 2009; Masi et al., 2013; Caracuta et al., 2016; Baton et al., 2017; Audiard et al., 2021).

The assessment of past carbonisation temperatures is therefore mandatory before using $\delta^{13}C$ as a potential climate proxy. Through experimental charring experiments, it has been demonstrated that the carbon content (%C) is correlated to heating temperatures up to 600 °C (Ferrio et al., 2006). Following this correlation, %C has been classically used to assess the carbonisation degree to which archaeological charcoals were subjected (Ferrio et al., 2006). With time and related post-depositional processes, charcoals are oxidised leading to an increase in oxygen (O) content (Wiedner et al., 2015). In turn, oxidation can yield a relative decrease in %C and therefore, an underestimation of past heating temperatures (Mouraux et al., 2022). Raman spectroscopy and relative derived parameters (notably the H_D/H_G ratio, the Raman thermometer; Deldicque et al., 2016), were proposed as an alternative method to determine heating temperatures. The H_D/H_G ratio is related to the carbon structural order and has been used to assess heating temperature from 400 to 1200 °C (Deldicque et al., 2016; Mouraux et al., 2022). Nonetheless, the impact of post-depositional processes on this Raman thermometer remains poorly constrained and understood. Lambrecht et al. (2021) were the first to present evidence for the modification of the the H_D/H_G ratio with post-depositional processes. Following this, Deldicque et al. (2023) provided additional insight by suggesting that chemical oxidation could enhance the H_D/H_G ratio, leading in turn to a possible overestimation of heating temperatures. To date, these studies have been based on a strong hypothesis, namely that the chemical structure of experimental charcoals was fully representative of that of the archaeological charcoals before they were subjected to post-depositional processes. To validate their findings and possibly provide new insights to understand changes in the Raman spectra as a consequence of post-depositional processes, additional investigations in which the chemical structure of charred wood is known are still required.

Post-depositional processes also involve inorganic and organic contaminations, which are likely to alter $\delta^{13}C$ values and therefore bias $\delta^{13}C$-based paleoclimate reconstruction. As an illustration, minor levels of contamination by carbonates can have a significant impact on $\delta^{13}C$ values (Vaiglova et al., 2014). With aging, charcoals in soils and sediments are subjected to biological or abiotic oxidation/adsorption, implying a rise in carboxylic/carboxylate functional groups (COOH/COO^-) and phenolic moieties at their surface (Wiedner et al., 2015; Zeba et al., 2022). Microbial biofilm and colonies may also develop on the surface of charcoals (Hockaday et al., 2006; Yan et al., 2023). For several decades, studies have highlighted the role of exogenous OM, in particular "humic substances", in modifying the $\delta^{13}C$ values determined in charcoals (DeNiro and Hastorf, 1985; Ascough et al., 2011; Vaiglova et al., 2014). To avoid such exogenous OM, archaeological charcoals are usually subjected to a chemical pre-treatment, the "Acid-Base-Acid" (ABA) procedure (Bird et al., 2014). However, the ABA procedure can lead to the destruction of studied charcoals. Vaiglova et al. (2014) suggested that $\delta^{13}C$ does not change when the humic acid concentration is lower than 10 % as revealed by Fourier-transform infrared spectroscopy (FTIR). Following this, they proposed the use of an acid-only procedure (0.5 M HCl for 30 min at 80 °C) to (i) remove carbonates as exogenous OM was considered to be negligible and (ii) avoid sample destruction. However, this approach encounters several problems. First, it has been demonstrated that humic substances do not occur naturally in soils and sediments and are now considered as being the by-product of alkali extraction (Kleber and Lehmann, 2019). Second, focusing on the occurrence of humic substances implies that additional sources of exogenous OM can be neglected. Third, wood charcoals present a high microporosity (Hossain et al., 2020). This high microporosity yields a large specific surface area, which can profoundly modify the interaction between the charcoal surface and exogenous OM through oxidation, adsorption and coating (Hagemann et al., 2017; Weng et al., 2022; Zeba et al., 2022). Taken together, these issues suggest the need to better constrain the effect of exogenous OM – independently of humic substances – on $\delta^{13}C$ measured on aged wood charcoals. This is a prerequisite in order to adapt future pre-treatments so that they respect the physical integrity of archaeological charcoals.

Our aims were therefore to evaluate the effects of post-depositional processes on the direct use of (i) Raman spectroscopy to assess past heating temperatures and of (ii) $\delta^{13}C$ isotope composition as a past climate/environmental proxy in archaeological charcoals. To this end, following a netbag experiment aiming to simulate post-depositional processes, charcoals from oak (*Quercus petraea*) and pine (*Pinus sylvestris*) were buried in vermicompost for 6 months. Changes in the chemical structure and isotope composition of the charred woods were then determined by combining elemental and isotope analyses (C, H, N, O, and $\delta^{13}C$), Raman spectroscopy, Rock-Eval® thermal analysis, and FTIR spectroscopy.

2. Material and methods

2.1. Studied charcoals and incubation

Charcoals were produced from oak (*Quercus petraea)* and pine (*Pinus sylvestris)* wood disks. Oak and pine charcoals are commonly observed in temperate Northern Hemisphere archaeological settings (Baton et al., 2017; Audiard et al., 2021). After drying, each disk (Ø ca. 7 cm; thickness: 2 cm) was wrapped in aluminium foil and placed in a muffle furnace set at 400 °C (1 h) and 600 °C (30 min) leading to the formation of charcoals respectively named oak-400 and pine-400 on the one hand, and oak-600 and pine-600 on the other hand. Charcoals were produced at 400 and 600 °C, which correspond to carbonisation temperatures usually estimated in archaeological charcoals (Cohen-Ofri, 2006; Ferrio et al., 2006). The charcoals were then crushed and sieved. Charcoals ranging in size between 1 and 2 mm were placed in nylon netbags (pore diameter size = 37 μm; 3 replicates) incubated in vermicompost (carbon and nitrogen content: 22 and 1.6 %, respectively) for 2, 4, 8, 16, and 32 weeks (at room temperature, ca. 20 °C). Using netbags with such a pore diameter size avoid cross-contamination of charcoals by particulate OM (Khan et al., 2017). In this study, vermicompost was not used as an analogue of archaeological soils/sediments but rather as a substrate enriched in OM favouring the establishment of microbial communities and consequently, modifications of the chemical structure of studied charcoals.

Vermicompost – previously homogenised through manual mixing – and nylon netbags were placed in aluminium containers and were kept at a moisture content of ca. 25 % (wt.) during the incubation experiment. Each week, aluminium containers were opened and their mass measured in order to determine changes in the moisture content. Subsequently, MilliQ water was added weekly to compensate this mass loss and keep moisture content constant.

After each incubation, nylon bags were opened allowing to directly retrieve charcoals, which were then crushed and sieved to obtain a powder. All analyses were then conducted on these powdered charcoals. Results of elemental and ^{13}C isotope composition, FTIR and Raman spectroscopy, and Rock-Eval® thermal analyses determined before incubation on the studied charcoals are presented in the supplementary information.

2.2. Elemental analyses

The elemental composition of the charcoals was determined with a Flash 2000 CHNS-O analyser. For each sample, 0.15–0.2 mg and 1.5–2 mg of powdered charcoals were put in tin and silver capsules to determine the C, H and N contents (% wt.) on the one hand, and the O content on the other hand. 2,5-Bis(5-*tert*-butyl-2-benzo-oxazol-2-yl) thiophene (BBOT) was used as an internal standard for the determination of C, H and N contents while cystine was used for the determination of the O content. Mean C, H and N contents of ca. 72.75 ± 0.45 %, 6.06 ± 0.07 % and 6.33 ± 0.04 % were determined on the BBOT standard. A mean O content of a. 26.34 ± 0.07 % was determined on cystine standard.

2.3. ^{13}C isotope analyses

For each sample, ca 0.3 µg of powdered charcoal was put in a tin capsule for analysis. The ^{13}C isotope composition was determined with an elemental analyser (Thermo Fisher Scientific Flash, 2000) coupled with an isotope ratio mass spectrometer (Thermo Fisher Scientific Delta V advantage). Uncharred oak powder, pure cellulose (IAEA-CH-3) and IRMS Reference Material (EMA P2) were used as internal standards (analytical error less than 0.1 ‰). All results were expressed in per mil (‰) in accordance with the international standard V-PDB (Vienna Pee Dee Belemnite).

2.4. Rock-Eval® thermal analysis

Rock-Eval® thermal analyses using a "6 Turbo" device (RE6) were conducted on charcoals to assess whether post-depositional processes lead to quantitative modifications of the chemical structure of studied charcoals. RE6 thermal analysis is conducted in two stages: a pyrolysis stage (under N_2 flow) followed by a combustion stage. In this study, we will focus only on the pyrolysis stage, as described below. First, the studied charcoals were subjected to an isothermal pyrolysis at 300 °C held for 3 min. Second, the pyrolysis temperature was increased at a rate of 25C/min up to 800 °C. During pyrolysis, the emission of hydrocarbons (HC) was continuously measured with a flame ionization detector (S1 and S2, respectively, in mg HC/g of the sample). The amount of HC released during the first isothermal pyrolysis at 300 °C is called the "S1 parameter" (Fig. 1). The amount of HC released from 300 to 800 °C is called the "S2 parameter". Following the analyses of pyrograms, we

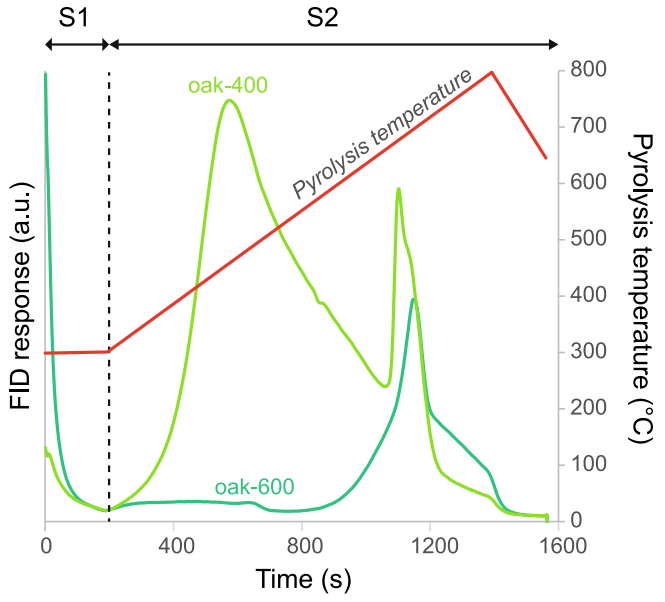

Fig. 1. Raw Rock-Eval® thermograms determined in oak charcoals produced at 400 and 600 °C.

computed the $S2_{300\text{-}500}$ and $S2_{500\text{-}800}$, which correspond to the integration of HC emissions in the temperature range indicated in the subscript. From 300 to 800 °C, emissions of HC reached a maximum intensity at a specific temperature, the TpkS2. The CO and CO_2 released during pyrolysis were also continuously monitored during pyrolysis with an infrared spectrometer. The amount of CO_2 released between 300 and 400 °C is called the "S3 parameter". In contrast to the S2 parameter, the S3 parameter is computed in a narrower range of pyrolysis temperature to avoid interference related to the thermal decomposition of inorganic materials such as carbonate (Espitalié et al., 1977; 1985).

2.5. Fourier-transform infrared spectroscopy

Modification of the chemical structure of charcoal samples by post-depositional processes was investigated by infrared spectroscopy with a Bruker Tensor 27 FTIR spectrometer. Powdered charcoal samples were first placed onto the germanium crystal. FTIR spectra were acquired from 4000 to 600 $cm^{-1,}$ with 64 scans at a 4 cm^{-1} resolution. FTIR spectra were corrected for CO_2, water vapour and ATR correction (Opus software). FTIR spectra were normalized to determine the intensity of the peaks occurring at ca. 1710–1740 cm^{-1} (Aromatic carbonyl/carboxyl C-O stretching and C = O assigned to carbonyl/carboxyl groups; hereafter called "Carbo."), 1600–1610 cm^{-1} (Aromatic C = C ring stretching, assigned to aromatic groups; hereafter called "Aro."), 1450–1460 cm^{-1} (CH bending vibrations, assigned to aliphatics; hereafter called "Aliph."), 1250–1260 cm^{-1} (Aromatic CO– and phenolic –OH stretching, assigned to phenols; hereafter called "Pheno.") and 1040–1050 cm^{-1} (Aliphatic ether C–O– and alcohol C–O stretching; assigned to polysaccharides: hereafter called "Poly."). Assignments of functional groups were done following Guo and Bustin (1998) and Solomon et al. (2005). Following the intensity of these peaks, the ratios Carbo./Aro., Aliph./Aro., Pheno./Aro. and Poly./Aro. were determined.

2.6. Raman spectroscopy

The aromatic structure of the charcoals was studied by Raman spectroscopy, performed using a HR800 Horiba Jobin Yvon spectrometer equipped with a 514.5 nm green laser. The laser was focused on the target with an Olympus 50 × objective (long working distance). The Raman spectroscope was first calibrated with a silicon crystal before the analytical session. The use of a 600 line/mm grating gives a spectral resolution of about 3 cm^{-1} and allows a large spectral window to be acquired in a single measurement. A laser power below 1 mW was applied on the samples to avoid thermal alteration during spectrum acquisition (Everall et al., 1991). Spectrum acquisition was achieved with an exposure time of 60 s. For each sample, the Raman shift intensity in the 600 to 2300 cm^{-1} spectral window was determined. This spectral window includes the first-order disorder (D) and graphite (G) bands. After linear baseline correction, two Raman-derived parameters were computed: the A_D/A_G and the H_D/H_G ratios corresponding to (i) the ratio between the integrated D (between 1000 and 1500 cm^{-1}) and G areas (between 1500 and 1800 cm^{-1}) and (ii) the ratio between the maximum intensity of the D and G bands, respectively (Fig. 2).

2.7. Statistics

Uncertainties presented in Figures and Tables are standard errors. The significance of the changes in the studied properties of the charcoals was evaluated by the non-parametric Kruskal-Wallis test followed by a Dunn's post-hoc test to allow pairwise comparison (three replicates). Charcoals incubated for 2 weeks were used as a reference to assess the effect of incubation on the chemical structure with time. Statistical analyses were performed with XLStat-Pro (v2010 AddinSoft) to test for significant modifications (p-value < 0.05) of studied parameters across treatment time for each type of charcoal (Five groups corresponding to each incubation time, three replicates in each group).The following

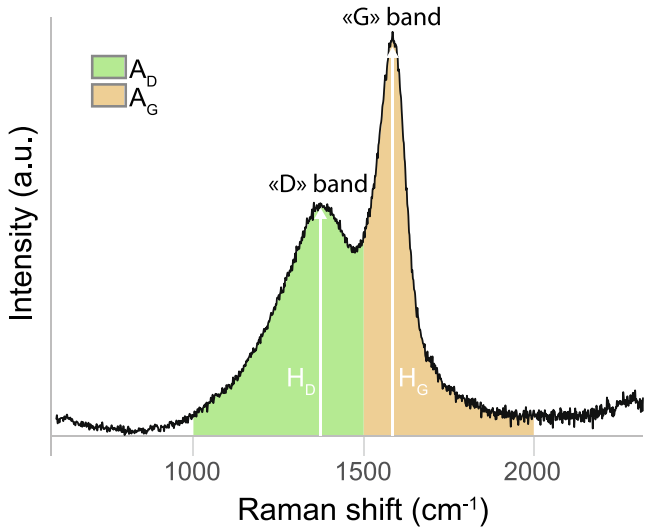

Fig. 2. Raman spectrum of pine-400 and Raman-derived parameters.

results and discussion sections only deal with results that are significantly different across replicates analysed at different time incubation.

3. Results

3.1. Elemental analyses

From 2 to 32 weeks of incubation, an overall decrease in the C/N ratio was observed at the end of the incubation experiment in all the studied charcoals. In oak-400 and pine-400, C/N ratios of 291 ± 31 (S.E.) and 240 ± 32 were determined after 2 weeks of incubation while they exhibited a value of 170 ± 3 and 162 ± 13 after 32 weeks of incubation (Fig. 3). In oak-600 and pine-600, C/N was about 272 ± 20 and 260 ± 23, respectively, after 2 weeks of incubation (Fig. 3). After 32 weeks, they declined to 172 ± 3 and 138 ± 9 (Fig. 3).

No effect was recorded on the H/C ratio determined in oak-400 and pine-600. In pine-400, an H/C ratio of 0.057 ± 0.002 was determined after 2 weeks of incubation (Fig. 3). After 16 and 32 weeks of incubation, the H/C ratio was enhanced to 0.065 ± 0.001 and 0.064 ± 0.001 in pine-400 (Fig. 3). In oak-600, an H/C ratio of 0.029 (S.E. < 0.001) was determined at the beginning of the incubation experiment. The H/C ratio then decreased slightly to 0.027 ± 0.001 in oak-600 incubated for 4 and 16 weeks (Fig. 3).

The effects of incubation on the O/C ratio were recorded only in oak and pine formed at 400 °C. After 2 weeks of incubation, O/C ratios of 0.26 ± 0.01 and 0.24 ± 0.01 were determined in oak-400 and pine-400, respectively (Fig. 3). In oak-400, a decrease in the O/C ratio to 0.24 (S.E < 0.01) was observed after 32 weeks of incubation. In pine-400, a slight increase in the O/C ratio up to 0.025 ± 0.01 was observed after 16 and 32 weeks of incubation.

3.2. Rock-Eval® thermal analyses

The results from RE6 analyses are summarized in Table 1. In oak-400, pine-400, oak-600 and pine-600, the S1 parameter exhibited values of 0.8 ± 0.02, 1.1 ± 0.02, 1.5 ± 0.03 and 1.5 ± 0.03 mg HC/g after 2 weeks of incubation, respectively. In oak-400, S1 increased to 1.1 ± 0.1 and 1.5 ± 0.1 after 8 and 16 weeks of incubation while an enhancement of S1 to 2.6 ± 0.01 was observed in pine-400 after 8 weeks. In oak-600, no clear effect was observed on S1 while it decreased to 0.5 ± 0.3 in pine-600 after 32 weeks.

In oak-400, pine-400, oak-600 and pine-600, the S2 parameter displayed values of 38.1 ± 0.2, 58.1 ± 6.7, 1.8 ± 0.2 and 5.3 ± 2.0 mg HC/g after 2 weeks of incubation, respectively. No effect of incubation on S2

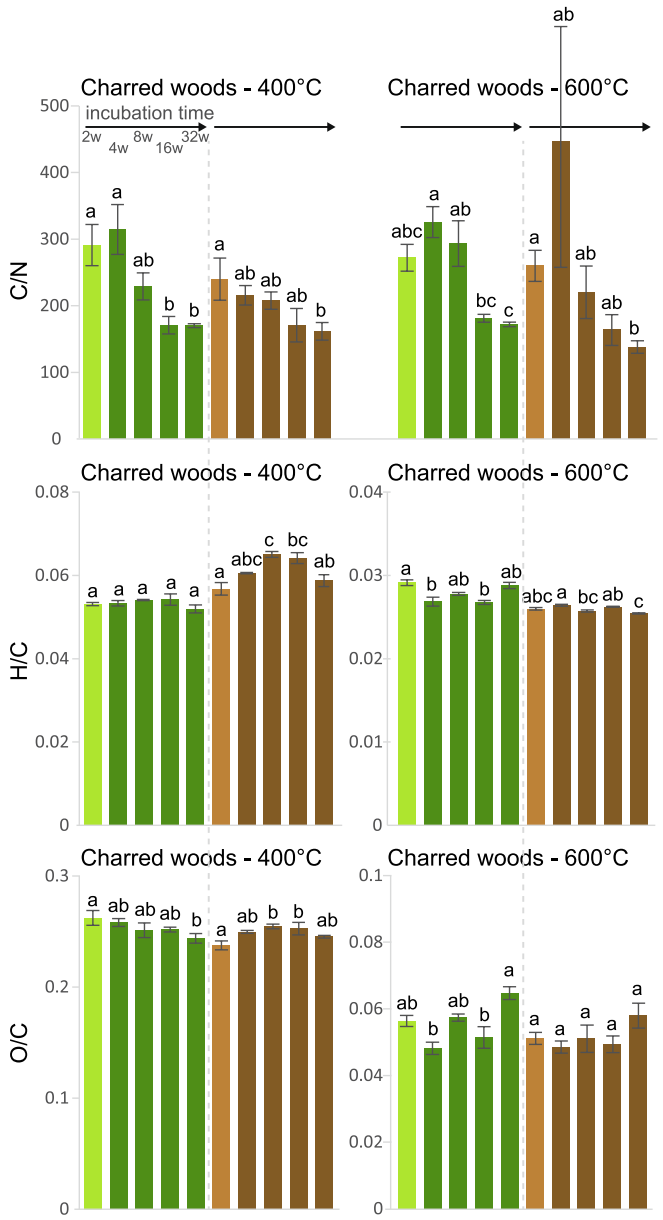

Fig. 3. Mean C/N, H/C and O/C ratios determined in oak-400, pine-400, oak-600 and pine-600 incubated for 2, 4, 8, 16 and 32 weeks. Green and brown bars correspond to oak and pine charcoals, respectively. Light green and light brown indicate the elemental composition of oak and pine charred woods determined at 2 weeks of incubation, a time at which the effects of post-depositional processes were minor. Dark green and dark brown indicate parameters determined after 2 weeks of incubation. Error bars correspond to standard errors (SE). Different letters denote significant differences at *p*-value ≤ 0.05. (For interpretation of the references to colour in this figure legend, the reader is referred to the web version of this article.)

was observed in oak-400, oak-600 and pine-600. In pine-400, S2 increased to 91.7 ± 2.6 and 86.6 ± 3.1 mg HC/g after 8 and 16 weeks of incubation, respectively. This increase was related to (i) a rise in the amount of HC compounds released between 300 and 500 as evidenced by $S2_{300\text{-}500}$ and (ii) a reduction in TpkS2 at the same incubation time. No effects were observed on $S2_{500\text{-}800}$ except in oak-400 in which it decreased from 14.8 ± 0.4 to 13.2 ± 0.2 mg HC/g between 2 weeks to 8 weeks of incubation.

In oak-400, pine-400, oak-600 and pine-600, the S3 parameter displayed values of 11.7 ± 0.1, 10.3 ± 0.3, 7.0 ± 0.3 and 6.0 ± 0.2 mg CO_2/g at the beginning of the incubation experiment, respectively.

Contrasted results were observed in the studied charcoals. In oak-400, S3 increased to 13.1 ± 0.1 and 13.0 ± 0.5 mg CO_2/g after 4 and 36 weeks of incubation. In pine-400 and pine-600, S3 decreased to 9.1 ± 0.1 and 4.9 ± 0.4 mg CO_2/g after 4 and 16 weeks, respectively. In oak-600, S3 decreased to 5.9 ± 0.2 and 6.0 ± 0.2 mg CO_2/g at 8 and 32 weeks of incubation, respectively.

3.3. Fourier-transform infrared spectroscopy

In oak-400, only the Aliph./Aro. ratio presented a modification with incubation. The Aliph./Aro. ratio decreased from 0.71 ± 0.02 to 0.65 ± 0.01 after 32 weeks of incubation (Table 2). In pine-400, the Aliph./Aro., Pheno./Aro. and Poly./Aro. ratios displayed values of 0.69, 0.69 and 0.14, respectively, at the beginning of the experiment. After 8 and 16 weeks of incubation, the Aliph./Aro. and Pheno./Aro. ratios increased up to 0.80 ± 0.02 and 0.90 ± 0.02 in pine-400 (Table 2). In oak-600, no effect was observed on the Aliph./Aro. and Poly./Aro. ratios in comparison to the values determined after 2 weeks of incubation (Table 2). At the beginning of the experiment, Carbo./Aro. and Pheno./Aro ratios of 0.49 ± 0.08 and 0.69 ± 0.04 were determined in oak-600, respectively (Table 2). These two ratios respectively reached 0.34 ± 0.01 and 0.81 ± 0.04 after 4 weeks of incubation. In pine-600, incubation did not result in any significant change in the Aliph./Aro. ratio (Table 2). Presenting a value of 0.27 ± 0.01 after 2 weeks of incubation, the Carbo./Aro. ratio increased by up to 0.34 ± 0.02 after 4, 8 and 16 weeks of incubation in pine-600. The Pheno./Aro ratio was 0.75 ± 0.01 after 2 weeks of incubation while it reached a value of 0.83 ± 0.02 after 36 weeks of incubation. Finally, the Poly./Aro. ratio determined in pine-600 was 0.16 ± 0.01, 0.38 ± 0.01 and 0.30 ± 0.04 after 2, 4 and 32 weeks of incubation (Table 2).

3.4. Raman spectroscopy

While several significant changes with incubation time were observed in the A_D/A_G and/or the H_D/H_G ratios determined in oak-400, pine-400 and oak-600, no obvious effect was observed on pine-600 (Fig. 4). At 2 weeks of incubation H_D/H_G ratios of 0.53 ± 0.01, 0.55 ± 0.02 and 0.62 ± 0.00 were determined in oak-400, pine-400 and oak-600, respectively (Fig. 4). At the same incubation time, A_D/A_G ratios of 1.11 ± 0.0, 1.10 ± 0.03 and 1.4 ± 0.01 were determined in oak-400, pine-400 and oak-600, respectively (Fig. 4). In oak-400, H_D/H_G and A_D/A_G ratios increased by up to 0.61 ± 0.01 and 1.23 ± 0.01, respectively after 16 weeks of incubation. In pine-400, the opposite pattern was observed (Fig. 4). H_D/H_G and A_D/A_G ratios, respectively, decreased by up to 0.50 ± 0.00 and 0.96 ± 0.04 after 32 weeks of incubation. In oak-600, no changes in the H_D/H_G ratio were observed although a slight increase in the A_D/A_G ratio up to 1.45 ± 0.02 was observed after 4 and 16 weeks of incubation (Fig. 4).

3.5. ^{13}C stable isotope composition

At 2 weeks of incubation, $\delta^{13}C$ values of −29.1 ± 0.2, −26.2 ± 0.0, −28.9 ± 0.2 and −26.4 ± 0.1 ‰ were determined in oak-400, pine-400, oak-600 and pine-600, respectively (Fig. 5). While no changes were observed with incubation time in oak-400, a slight increase was observed in pine-400. Occurring after 4, 16 and 32 weeks of incubation, the reduction in $\delta^{13}C$ reached 0.3 ‰ (Fig. 5). In contrast to pine-400, $\delta^{13}C$ values decreased in oak-600 and pine-600 after 4 and 36 weeks of incubation. In oak-600, the decline in $\delta^{13}C$ was 0.5 ‰ while it was 0.2 ‰ in pine-600 (Fig. 5).

4. Discussion

4.1. Identification of exogenous organic matter

Although a few changes in the chemical composition of oak-400, oak-600 and pine-600 were recorded with incubation time, they cannot be used to define an overall scheme for exogenous OM in these charcoals. Most of the chemical changes that occurred during incubation were observed in pine-400. Interestingly, following plant species and heating temperatures, pine-400 can be seen as an analogue of numerous archaeological charcoals used for paleoclimate reconstruction (Ferrio et al., 2006; Aguilera et al., 2009). In pine-400, slight rises in O/C and H/C ratios were observed with incubation time (Fig. 1 and Fig. 6).

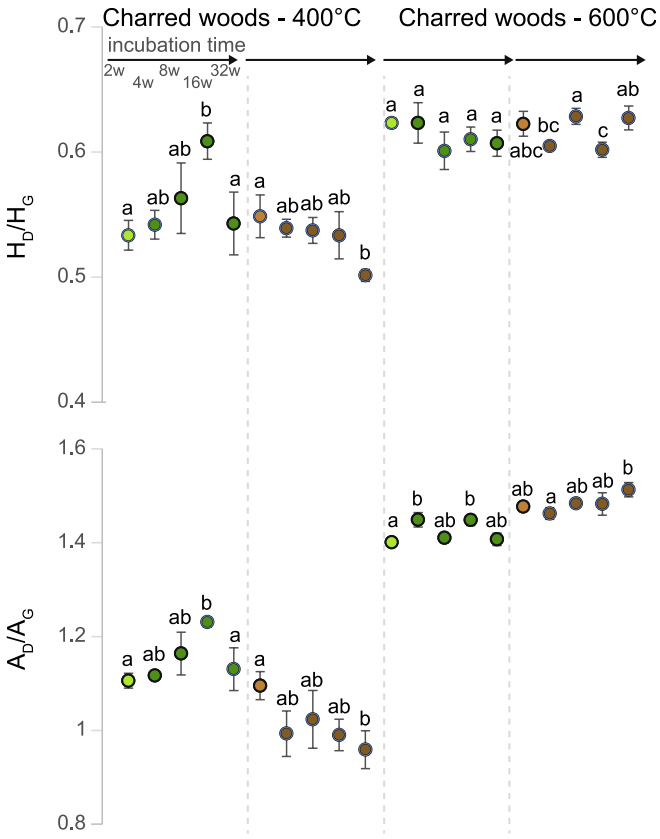

Fig. 4. Mean H_D/H_G and A_D/A_G determined by Raman spectroscopy in oak-400, pine-400, oak-600 and pine-600 incubated for 2, 4, 8, 16 and 32 weeks. Green and brown circles correspond to oak and pine charcoals, respectively. Light green and light brown indicate the H_D/H_G and A_D/A_G determined in oak and pine charred woods determined at 2 weeks of incubation, a time at which the effects of post-depositional processes were minor. Dark green and dark brown indicate parameters determined after 2 weeks of incubation. Error bars correspond to standard errors (SE). Different letters denote significant differences at p-value ≤ 0.05. (For interpretation of the references to colour in this figure legend, the reader is referred to the web version of this article.)

Such a rise in the O and H contents could be assigned to an effect of oxidation and adsorption of organic compounds, which have been demonstrated to modify the elemental composition of charcoals (Wiedner et al., 2015; Zeba et al., 2022). However, RE6 provides an alternative explanation here. Parameter S1, which is related to free hydrocarbonaceous and thermodesorbable OM (Delarue et al., 2018; Romero-Sarmiento et al., 2016), does not support a potential rise in the adsorption of organics at the surface of pine-400. Interestingly, the rise in H/C was associated with an enhancement of the S2 parameter in pine-400 (Fig. 6), which is used to assess the Hydrogen Index, a proxy of the H/C atomic ratio in geological organic materials (Espitalié et al., 1977). Parameter S2 quantifies HC emissions related to the thermal cracking of organic compounds that are covalently bonded within a macromolecular structure (Vandenbroucke et al., 1988; Sykes and Snowdon, 2002).

As HC emissions correspond to the thermal cracking of covalently bonded OM, a rise in S2 therefore suggests that the additional amount of H observed in pine-400 does not originate from adsorption but rather

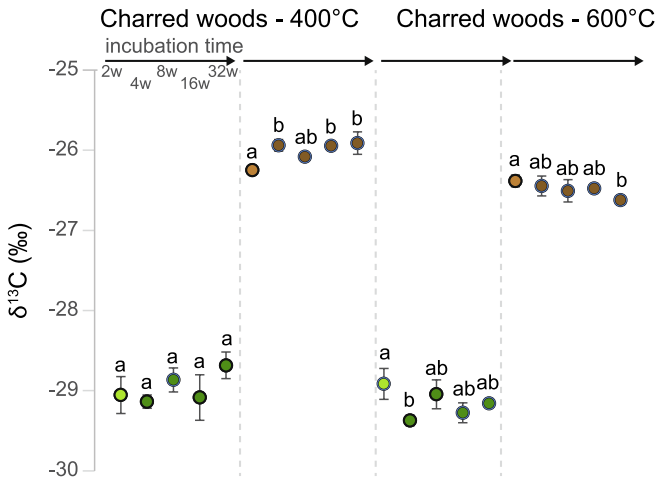

Fig. 5. Mean $\delta^{13}C$ determined in oak-400, pine-400, oak-600 and pine-600 incubated for 2, 4, 8, 16 and 32 weeks. Green and brown circles correspond to oak and pine charcoals, respectively. Light green and light brown indicate the $\delta^{13}C$ determined in oak and pine charred woods at 2 weeks of incubation, a time at which the effects of post-depositional processes were minor. Dark green and dark brown indicate parameters determined after 2 weeks of incubation. Error bars correspond to standard errors (SE). Different letters denote significant differences at p-value ≤ 0.05. (For interpretation of the references to colour in this figure legend, the reader is referred to the web version of this article.)

from another source of OM presenting a macromolecular structure. In pine-400, this additional source of OM implies a higher contribution of HC released prior to 500 °C and a lowering of TpkS2 (Table 1; Kruskal-Wallis p-value = 0.001) by up to 20 °C (Table 1; Kruskal-Wallis p-value = 0.001). Such a lowering of TpkS2 likely indicates the appearance of a new thermolabile organic pool with incubation time.

Previous netbag experiments have described a microbial colonization at the surface of charcoals (Khan et al., 2017). Through microbial colonization and the production of an extracellular polymeric matrix, biofilm can develop at the surface of charcoals (Hockaday et al., 2006; Yan et al., 2023). Biofilms are enriched polysaccharides (Naseem et al., 2018) and can consist of a source of exogenous OM that coats the surface of charcoals. Here, an overall decrease in the C/N ratio was observed in all the studied charcoals with incubation time (Fig. 3). This reduction indicates additional N exogenous inputs. These N exogenous inputs can originate from organic compounds as well as inorganic compounds such as NO_3^- or NH_4^+ that are likely adsorbed onto the charcoal surface (Fidel et al., 2018). No organic or inorganic N was observed with FTIR absorption bands, precluding their identification. Nonetheless, it is worth mentioning that C/N variations are not correlated with any variables measured on the studied charcoals. This suggests that N variations are not related to organics but rather to an inorganic N source such as nitrate. Such a scenario is in line with recent results, which describe a nitrate enrichment in the organic coating formed at the surface of charcoals (Hagemann et al., 2017). In addition, pine-400 presents higher polysaccharide contents as revealed by FTIR spectra. This is expected in the formation of an organic coating related to an extracellular polymeric matrix. Taken all together, the chemical proxies mainly argue for an exogenous OM of pine-400 by a microbial-derived OM. While the organic coating likely explains most of the chemical modifications in pine-400, the simultaneous effect of oxidation seems very limited as no changes in carboxylic and phenolic functional groups were recorded in pine-400 (Table 2; Fig. 6).

4.2. *Short-term post-depositional processes can bias the estimation of past heating temperatures using Raman thermometers*

The aromatic structure of charcoals can be probed with Raman spectroscopy especially by using the geometrical features of the D and G bands observed in the first-order region of the Raman spectra (Ferralis et al., 2016). Observed at ca. 1380 cm^{-1} (Fig. 2), the D band exhibits a complex shape including several sub-bands related to the absence/presence of aliphatics, heteroatoms, structural defects, and vacancies (Rouzaud et al., 2015; Ferralis et al., 2016). The G-band (ca. 1595 cm^{-1}) is related to the vibrations of C = C bonds within graphene-like clusters (Ferralis et al., 2016). As both the A_D/A_G and H_D/H_G ratios increase with the formation and growth of aromatic clusters that occur with heating (Deldicque et al., 2016; Mouraux et al., 2022), these Raman-derived parameters have been used to estimate the heating temperatures to which the charcoals had been subjected (Deldicque et al., 2016; Deldicque and Rouzaud, 2020, Mouraux et al., 2022). Up to now, little is known about the effect of post-depositional processes on these Raman thermometers. Here, no effect of incubation time was observed on H_D/H_G and A_D/A_G ratios (Kruskal-Wallis p-value > 0.05 for all studied charcoals.). Nonetheless, a slight increase or alternatively, decrease in H_D/H_G and A_D/A_G ratios was recorded at certain incubation times in oak-400, pine-400 and oak-600 (Fig. 4).

Investigating the effect of oxidation on carbonised charcoals and bones, Deldicque et al. (2023) proposed that oxidation leads to the removal of aliphatic chains and heteroatoms. Following this, they further suggested a relative increase in the proportion of polyaromatic rings with oxidation, which would increase the intensity of the D band. In the present study, the occurrence of oxidation is unlikely, or at least very limited, as it was not straightforwardly recorded. Instead of an enrichment in O, a relative depletion in O was observed in oak-400 and oak-600 (Fig. 3 and Fig. 6). In oak-400, this depletion was only observed at 32 weeks of incubation (Fig. 3). Decreases in the O/C ratio suggest a preferential degradation of oxygen-enriched compounds in oak-400 and oak-600. Used as a proxy of the O content in coal and other thermally altered geological material (Copard et al., 2002), the S3 parameter does not confirm the observed decrease in O/C as it decreases and alternatively increases in oak-400 and oak-600, respectively, with incubation times (Fig. 3). A preferential biological degradation would yield a relative rise in the concentration of aromatic moieties. Consequently, this would lead to the rise in H_D/H_G and A_D/A_G ratios (Fig. 4), which "mimic" the effect of increased heating temperature. However, it is worth mentioning that further experimental investigations are still required to support or discount this hypothesis as this preferential degradation was not confirmed either by RE6 analyses or by FTIR spectroscopy. In contrast to oak-400 and oak-600, post-depositional processes in pine-400 led to a reduction in H_D/H_G and A_D/A_G ratios (Fig. 4), which likely implies an underestimation of past heating temperatures with these Raman thermometers. In this case, the occurrence of organic coating and potentially, the addition of amorphous carbon at the edge of the aromatic structure may have led to a relative decrease in the proportion of polyaromatic rings, leading in turn to a decrease in H_D/H_G and A_D/A_G ratios. Although additional experiments are required to fully understand the exact mechanism(s) leading to opposite changes in the Raman line shape as observed in oak and pine charcoals, this study provides additional insights to those evidencing/suggesting an overestimation of heating temperatures through an increase in the H_D/H_G ratio (Lambrecht et al., 2021; Deldicque et al., 2023).

4.3. *Effect of short-term post-depositional processes on $\delta^{13}C$ values: Implications for paleoclimate assessment*

Slight decreases in $\delta^{13}C$ were observed in oak-600 and pine-600 after 4 weeks and 36 weeks of incubation, respectively (Fig. 5). These modifications systematically occurred at a time when phenolics presented a higher relative intensity in FTIR spectra (Table 2). Such a rise in phenolics can be consistent with the observed decreases in $\delta^{13}C$ as they are known to be relatively depleted in ^{13}C in comparison to other compounds such as cellulose or hemicellulose (Czimczik et al., 2002; Turney et al., 2006; Ascough et al., 2008). Nonetheless, comparison with the

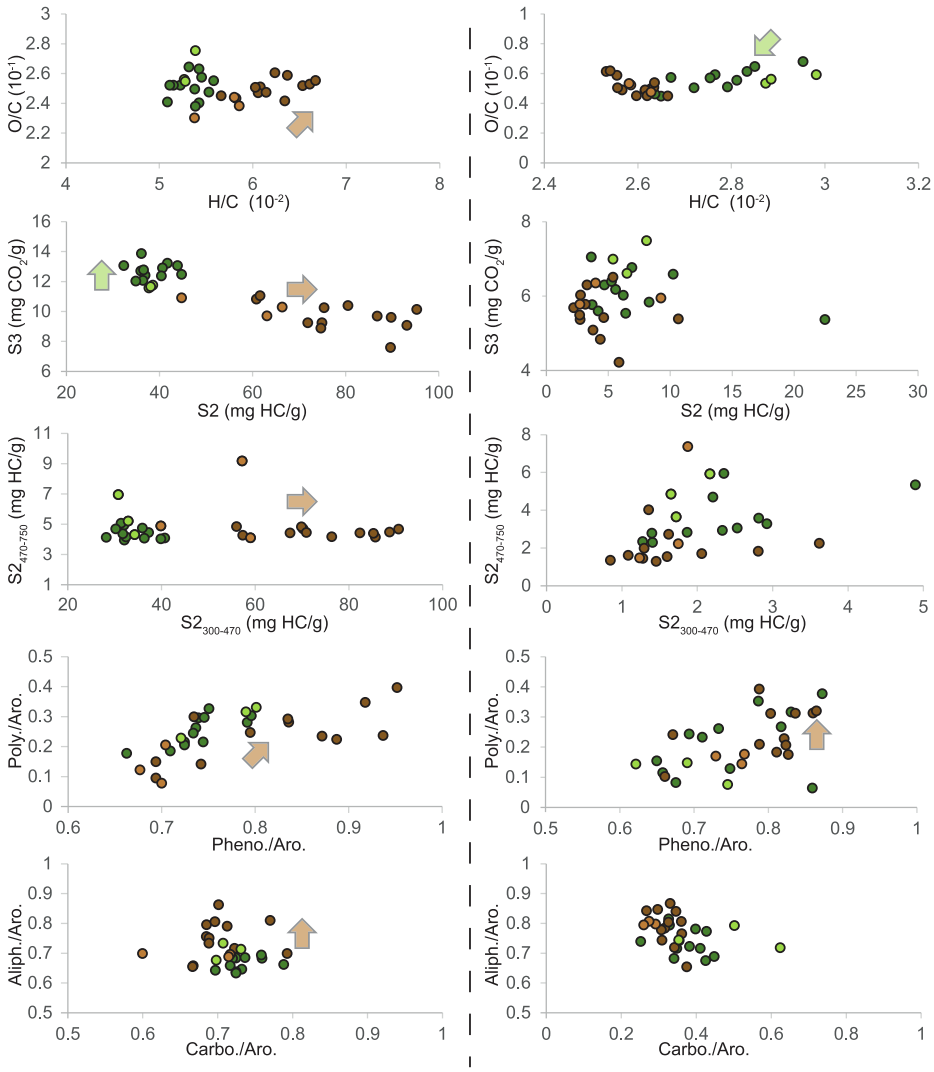

Fig. 6. Evolution of elemental composition, Rock-Eval® thermal analyses, and FTIR-derived parameters determined in oak-400, pine-400, oak-600 and pine-600 incubated for 2, 4, 8, 16 and 32 weeks. Each circle corresponds to a replicate. Green and brown circles correspond to oak and pine charcoals, respectively. Light green and light brown indicate parameters determined at 2 weeks of incubation, a time at which the effects of post-depositional processes were minor. Dark green and dark brown indicate parameters determined after 2 weeks of incubation. Occurrence of arrows indicate significant effect of incubation time (Kruskal-Wallis; *p*-value < 0.05). Horizontal arrows indicate significant effects on the variable related to the abscissa axis while vertical arrows indicate a significant effect on the variables related to the ordinate axis. Arrows at an angle indicate significant effects on the two variables. (For interpretation of the references to colour in this figure legend, the reader is referred to the web version of this article.)

$\delta^{13}C$ determined on these charcoals before incubation (supplementary information) suggests that observed modifications in $\delta^{13}C$ cannot be straightforwardly assigned to post-depositional processes.

In contrast to oak-600 and pine-600, a slight but significant increase of $\delta^{13}C$ was observed in pine-400 with incubation time (Fig. 5). Reaching a maximum value of ca. 0.34 ‰, this shift in $\delta^{13}C$ is consistent with the observed rise in polysaccharides and aliphatic compounds that are known to be enriched in ^{13}C in comparison to aromatic moieties. In addition, such a shift in $\delta^{13}C$ cannot be considered as negligible when comparing $\delta^{13}C$ values from charcoals sampled in different archaeological sites (Baton et al., 2017; Audiard et al., 2021). Indeed, although these charcoals may have been produced at a similar heating temperature, one cannot exclude potential discrepancies in the intensity of post-depositional processes, which are highly dependent on the physico-chemical properties of the surrounding soils or sediments. To avoid such a potential issue, pre-treatments –including the ABA treatment– are often applied on charcoals in order to minimise/exclude exogenous organic and inorganic contaminations. Negligible $\delta^{13}C$ changes were hypothesized when contamination by humic substances was lower than 10 % (Vaiglova et al., 2014). As stressed before, humic substances do not exist naturally in soils and sediments. Consistently, we did not observe any FTIR peaks that were related to these by-products of alkali extraction. In fact, only very subtle chemical variations were observed in FTIR spectra from pine-400 (Fig. 7) although it presented a significant ^{13}C contamination after a very short-term experiment in comparison to the residence time of archaeological charcoals from the Neolithic and Paleolithic.

These results suggest that pre-treatments dedicated to the removal of exogenous OM are still required even though FTIR spectroscopy does not reveal obvious changes in the chemical structure of charred woods. This conclusion does not mean that paleoclimate reconstructions based on the $\delta^{13}C$ measured on archaeological charcoals are biased in the absence of a pre-treatment dedicated to the removal of exogenous OM, since the use of an acid treatment to remove carbonate may also favour the hydrolysis of microbial residues, depending on the concentration of the acid and on the duration and temperature of the acidic treatment. Nonetheless, the efficiency of such a chemical treatment to remove exogenous OM, which can arise from several sources, must be properly

Table 1
Rock-Eval analysis-derived parameters (S1, S2, $S2_{300-500}$, $S2_{500-800}$, TpS2 and S3) determined in oak-400, pine-400, oak-600 and pine-600 incubated for 2, 4, 8, 16 and 32 weeks. Standard errors are indicated between brackets. Different letters denote significant differences at p-value ≤ 0.05.

		S1 (mg HC/g)	S2 (mg HC/g)	$S2_{300-500}$ (mg HC/g)	$S2_{500-800}$ (mg HC/g)	TpS2	S3 (mg CO_2/g)
oak-400	2w	0.8 (±0.02)a	38.1 (±0.2)a	23.3 (±0.6)a	14.8 (±0.4)a	471(±4)a	11.7 (±0.1)a
	4w	0.8 (±0.1)ab	38.2 (±3.0)a	24.7 (±2.8)a	13.5 (±0.2)ab	467(±8)a	13.1 (±0.1)b
	8w	1.1 (±0.1)bc	40.4 (±2.5)a	27.2 (±2.3)a	13.2 (±0.2)b	464(±4)a	12.5 (±0.1)ab
	16w	1.5 (±0.1)c	36.7 (±0.1)a	23.1 (±0.2)a	13.6 (±0.2)ab	476(±5)a	12.4 (±0.2)ab
	32w	0.9 (±0.2)abc	38.3 (±2.8)a	24.9 (±3.2)a	13.4 (±0.4)ab	475(±6)a	13.0 (±0.5)b
pine-400	2w	1.1 (±0.2)a	58.1 (±6.7)a	38.5 (±6.2)a	18.6 (±2.0)a	483(±8)a	10.3 (±0.3)a
	4w	1.3 (±0.1)a	73.8 (±1.0)abc	56.0 (±0.7)abc	17.8 (±0.3)a	467(±0)abc	9.1 (±0.1)b
	8w	2.6 (±0.1)b	91.7 (±2.6)c	74.8 (±2.3)c	16.9 (±0.3)a	459(±1)c	9.6 (±0.3)ab
	16w	1.5 (±0.2)ab	86.6 (±3.1)bc	70.3 (±2.8)bc	16.4 (±0.5)a	461(±1)bc	9.2 (±0.8)ab
	32w	1.3 (±0.2)a	65.9 (±4.7)ab	49.5 (±4.7)ab	16.4 (±0.4)a	475(±5)ab	10.7 (±0.2)a
oak-600	2w	1.5 (±0.3)ab	6.7 (±0.8)ab	1.1 (±0.2)a	5.5 (±0.6)a	713(±7)a	7.0 (±0.3)a
	4w	1.2 (±0.2)ab	4.7 (±1.1)b	1.2 (±0.2)a	3.5 (±0.8)a	722(±5)a	6.5 (±0.4)ab
	8w	0.8 (±0.2)a	5.7 (±1.3)ab	1.2 (±0.2)a	4.5 (±1.1)a	718(±5)a	5.9 (±0.2)b
	16w	2.4 (±0.4)b	12.8 (±5.0)a	3.3 (±0.7)b	9.5 (±4.7)a	634(±79)a	6.0 (±0.4)ab
	32w	0.6 (±0.1)a	6.0 (±0.4)ab	1.9 (±0.2)ab	4.0 (±0.3)a	724(±3)a	6.0 (±0.2)b
pine-600	2w	1.5 (±0.3)a	5.3 (±2.0)a	1.3 (±0.1)ab	4.0 (±1.9)a	732(±19)a	6.0 (±0.2)a
	4w	0.8 (±0.1)ab	3.4 (±1.0)a	0.9 (±0.1)b	2.6 (±0.9)a	750(±15)a	5.9 (±0.3)ab
	8w	1.0 (±0.2)ab	5.5 (±2.6)a	1.1 (±0.2)ab	4.4 (±2.5)a	739(±16)a	5.6 (±0.1)ab
	16w	1.5 (±0.2)a	4.8 (±0.6)a	2.5 (±0.4)a	2.3 (±0.2)a	480(±3)b	4.9 (±0.4)b
	32w	0.5 (±0.3)b	3.5 (±0.5)a	1.2 (±0.0)ab	2.3 (±0.4)a	465(±82)ab	5.7 (±0.4)ab

Table 2
FTIR absorption band intensity ratios (Aliph., Aro.. Carbo., Pheno., Poly., stand for aliphatics, aromatics, carbonyl/carboxyl groups, phenols and polysaccharides, respectively) determined in oak-400, pine-400, oak-600 and pine-600 incubated for 2, 4, 8, 16 and 32 weeks. Standard errors are indicated between brackets. Different letters denote significant differences at p-value ≤ 0.05.

		Aliph./Aro.	Carbo./Aro.	Pheno./Aro.	Poly./Aro.
oak-400	2w	0.71(±0.02)a	0.71(±0.01)a	0.77(±0.03)a	0.29(±0.03)a
	4w	0.67(±0.01)ab	0.74(±0.01)a	0.75(±0.02)a	0.25(±0.02)a
	8w	0.67(±0.02)ab	0.74(±0.01)a	0.74(±0.01)a	0.24(±0.03)a
	16w	0.68(±0.01)ab	0.72(±0.01)a	0.76(±0.02)a	0.29(±0.02)a
	32w	0.65(±0.01)b	0.74(±0.03)a	0.71(±0.02)a	0.22(±0.04)a
pine-400	2w	0.69(±0.00)a	0.68(±0.04)a	0.69(±0.01)a	0.14(±0.04)a
	4w	0.74(±0.02)ab	0.72(±0.04)a	0.77(±0.04)ab	0.21(±0.06)ab
	8w	0.79(±0.04)b	0.70(±0.01)a	0.87(±0.07)b	0.35(±0.03)b
	16w	0.80(±0.01)b	0.73(±0.02)a	0.90(±0.02)b	0.23(±0.00)ab
	32w	0.68(±0.03)a	0.67(±0.01)a	0.76(±0.04)ab	0.19(±0.05)ab
oak-600	2w	0.75(±0.02)ab	0.49(±0.08)a	0.69(±0.04)a	0.12(±0.02)a
	4w	0.78(±0.02)a	0.34(±0.01)b	0.81(±0.04)b	0.30(±0.09)a
	8w	0.70(±0.01)b	0.42(±0.02)ab	0.69(±0.03)a	0.18(±0.04)a
	16w	0.73(±0.03)ab	0.33(±0.04)ab	0.80(±0.05)ab	0.25(±0.07)a
	32w	0.74(±0.02)ab	0.40(±0.02)ab	0.72(±0.03)ab	0.23(±0.08)a
pine-600	2w	0.80(±0.00)ab	0.27(±0.01)a	0.75(±0.01)a	0.16(±0.01)a
	4w	0.83(±0.01)a	0.33(±0.02)b	0.82(±0.02)ab	0.38(±0.01)c
	8w	0.79(±0.04)ab	0.33(±0.02)b	0.82(±0.01)ab	0.29(±0.05)abc
	16w	0.72(±0.04)b	0.34(±0.02)b	0.72(±0.05)ab	0.19(±0.05)ab
	32w	0.81(±0.02)ab	0.30(±0.02)ab	0.83(±0.02)b	0.30(±0.04)bc

verified to avoid any misuse of $\delta^{13}C$ values for paleoclimate reconstruction. Indeed, although several studies showed that pre-treatment can lead to a modification of the $\delta^{13}C$ signature of archaeological charcoals, it is worth mentioning that none of them has proven to retrieve the initial isotope signature of the charcoal as the starting material is no longer available. Such a gap in current knowledge can be filled by taking advantage of current *in situ* investigations on the effect of biochar on soil functions, which has been conducted over decades. In such a view, these experiments may offer a valuable framework to test the effect of post-depositional processes as well as the use of pre-treatment(s) to minimise/avoid biases in using $\delta^{13}C$ to depict past climates as well as the Raman thermometer to determine carbonisation temperatures.

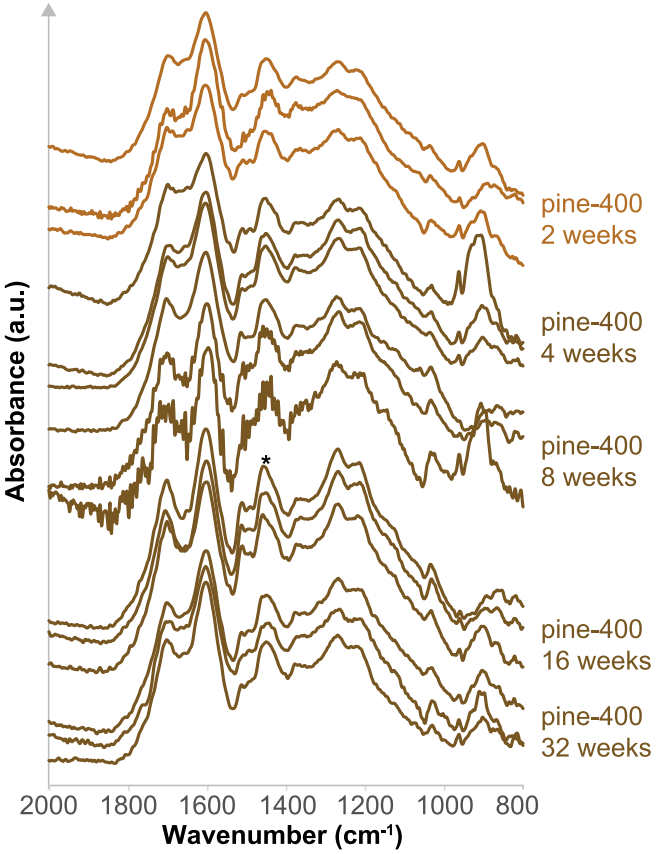

Fig. 7. FTIR spectra determined in pine-400 incubated for 2, 4, 8, 16 and 32 weeks.

5. Conclusion

Our aims were to assess the effects of post-depositional processes on the use of (i) Raman thermometers and of (ii) $\delta^{13}C$ as a past climate/environmental proxy when applied to archaeological charcoals. Following oxidation/adsorption and organic coating revealed by the combination of elemental composition, FTIR spectroscopy and Rock-

Eval® thermal analysis, contrasted effects on both Raman thermometers (under- and overestimation of heating temperatures) and $\delta^{13}C$ (enrichment or depletion in ^{13}C) were recorded across time in charred oak and pine woods formed at 400 and 600 °C. It is worth bearing in mind that these contrasted changes were observed in unfavourable conditions compared to archaeological charcoals since they were observed (i) only after a 6-month incubation, whereas archaeological charcoals can be subjected to post-depositional contamination for thousands of years and (ii) in a netbag experiment that intrinsically minimises chemical interactions with organic and mineral matter from the soil. By showing these contrasted responses of the Raman thermometer and of $\delta^{13}C$, this study suggests that further experimental investigations – especially on long-term incubation in which the initial chemical structure of the charcoals is fully controlled – are still required. Such experimental investigations are necessary to provide suitable methods to constrain the effect(s) of post-depositional processes on the determination of Raman thermometry and $\delta^{13}C$, which are prerequisites for the study of past climate/environmental conditions with archaeological charcoals.

CRediT authorship contribution statement

Frédéric Delarue: Writing – review & editing, Writing – original draft, Validation, Supervision, Project administration, Methodology, Investigation, Funding acquisition, Formal analysis, Data curation, Conceptualization. **Amir Ghavidel:** Writing – review & editing, Writing – original draft, Formal analysis, Data curation. **Katell Quénéa:** Writing – review & editing, Conceptualization. **Ludovic Bellot-Gurlet:** Writing – review & editing. **Eva Rocha:** Writing – review & editing. **Sylvie Coubray:** Writing – review & editing, Conceptualization. **François Baudin:** Writing – review & editing. **David Sebag:** Writing – review & editing. **Michel Lemoine:** Methodology, Formal analysis. **Emmanuel Aubry:** Methodology, Formal analysis. **Florence Savignac:** Formal analysis. **Alexa Dufraisse:** Writing – review & editing, Supervision, Project administration, Methodology, Funding acquisition, Conceptualization.

Declaration of competing interest

The authors declare that they have no known competing financial interests or personal relationships that could have appeared to influence the work reported in this paper.

Data availability

Data will be made available on Zenodo (10.5281/zenodo.11276298).

Acknowledgments

This work was supported by the Paris Ile-de-France Region through the Domaine d'intérêt majeur (DIM) programme: 'Matériaux anciens et patrimoniaux', The INSU EC2CO program, PEPS INEE and Action transverse MITI (Chantier scientifique Notre-Dame de Paris) are also acknowledged for financial support. This work also benefits from the financial support of the "ANR Agence Nationale de la Recherche" (CASIMODO project; ANR-20-CE03-0008). We are grateful to Mercedes Mendez-Millan (Alysés platform, IRD), Assia Hessani (Sorbonne Université PLASVO platform) and Christelle Anquetil (Sorbonne Université, GEORG platform) for stable carbon isotope composition, Raman spectroscopy and Fourier-transform infrared spectroscopy. Rock-Eval® is a trademark registered by IFPEN. We also acknowledge Elizabeth Rowley-Jolivet for English language editing. Full dataset is available on Zenodo (10.5281/zenodo.11276298).

Appendix A. Supplementary material

Supplementary data to this article can be found online at https://doi.org/10.1016/j.jasrep.2024.104672.

References

Aguilera, M., Espinar, C., Ferrio, J.P., Pérez, G., Voltas, J., 2009. A map of autumn precipitation for the third millennium BP in the Eastern Iberian Peninsula from charcoal carbon isotopes. J. Geochem. Explor. 102, 157–165. https://doi.org/10.1016/j.gexplo.2008.11.019.

Ascough, P.L., Bird, M.I., Wormald, P., Snape, C.E., Apperley, D., 2008. Influence of production variables and starting material on charcoal stable isotopic and molecular characteristics. Geochim. Cosmochim. Acta 72, 6090–6102. https://doi.org/10.1016/j.gca.2008.10.009.

Ascough, P.L., Bird, M.I., Francis, S.M., Lebl, T., 2011. Alkali extraction of archaeological and geological charcoal: Evidence for diagenetic degradation and formation of humic acids. J. Archaeol. Sci. 38, 69–78. https://doi.org/10.1016/j.jas.2010.08.011.

Audiard, B., Meignen, L., Blasco, T., Battipaglia, G., Théry-Parisot, I., 2021. New climatic approaches to the analysis of the middle Paleolithic sequences: Combined taxonomic and isotopic charcoal analyses on a Neanderthal settlement, Les Canalettes (Aveyron, France). Quat. Int. 593–594, 85–94. https://doi.org/10.1016/j.quaint.2020.11.042.

Baton, F., Nguyen Tu, T.T., Derenne, S., Delorme, A., Delarue, F., Dufraisse, A., 2017. Tree-ring δ13C of archeological charcoals as indicator of past climatic seasonality. A case study from the Neolithic settlements of Lake Chalain (Jura, France). Quaternary International 457, 50–59. 10.1016/j.quaint.2017.03.015.

Bird, M.I., Levchenko, V., Ascough, P.L., Meredith, W., Wurster, C.M., Williams, A., Tilston, E.L., Snape, C.E., Apperley, D.C., 2014. The efficiency of charcoal decontamination for radiocarbon dating by three pre-treatments – ABOX, ABA and hypy. Quat. Geochronol. 22, 25–32. https://doi.org/10.1016/j.quageo.2014.02.003.

Bonal, D., Pau, M., Toigo, M., Granier, A., Perot, T., 2017. Mixing oak and pine trees does not improve the functional response to severe drought in central French forests. Ann. For. Sci. 74, 72. https://doi.org/10.1007/s13595-017-0671-9.

Caracuta, V., Weinstein-Evron, M., Yeshurun, R., Kaufman, D., Tsatskin, A., Boaretto, E., 2016. Charred wood remains in the natufian sequence of el-Wad terrace (Israel): New insights into the climatic, environmental and cultural changes at the end of the Pleistocene. Quat. Sci. Rev. 131, 20–32. https://doi.org/10.1016/j.quascirev.2015.10.034.

Cohen-Ofri, I., Weiner, L., Boaretto, E., Mintz, G., Weiner, S., 2006. Modern and fossil charcoal: Aspects of structure and diagenesis. J. Archaeol. Sci. 33, 428–439. https://doi.org/10.1016/j.jas.2005.08.008.

Copard, Y., Disnar, J.R., Becq-Giraudon, J.F., 2002. Erroneous maturity assessment given by Tmax and HI Rock-Eval parameters on highly mature weathered coals. Int. J. Coal Geol. 49, 57–65. https://doi.org/10.1016/S0166-5162(01)00065-9.

Czimczik, C.I., Preston, C.M., Schmidt, M.W.I., Werner, R.A., Schulze, E.-D., 2002. Effects of charring on mass, organic carbon, and stable carbon isotope composition of wood. Org Geochem. 33, 1207–1223. https://doi.org/10.1016/S0146-6380(02)00137-7.

Delarue, F., Derenne, S., Sugitani, K., Baudin, F., Westall, F., Kremer, B., Tartèse, R., Gonzalez, A., Robert, F., 2018. What is the meaning of hydrogen-to-carbon ratio determined in Archean organic matter? Org Geochem. 122, 140–146. https://doi.org/10.1016/j.orggeochem.2018.05.013.

Deldicque, D., Rouzaud, J.-N., 2020. Temperatures reached by the roof structure of Notre-Dame de Paris in the fire of April 15th 2019 determined by Raman paleothermometry. Comptes Rendus. Géosci. 352, 7–18. https://doi.org/10.5802/crgeos.9.

Deldicque, D., Rouzaud, J.-N., Velde, B., 2016. A Raman – HRTEM study of the carbonization of wood: A new Raman-based paleothermometer dedicated to archaeometry. Carbon 102, 319–329. https://doi.org/10.1016/j.carbon.2016.02.042.

Deldicque, D., Rouzaud, J.-N., Vandevelde, S., Medina-Alcaide, M.Á., Ferrier, C., Perrenoud, C., Pozzi, J.-P., Cabanis, M., 2023. Effects of oxidative weathering on Raman spectra of charcoal and bone chars: consequences in archaeology and paleothermometry. Comptes Rendus. Géosci. 355, 1–22. https://doi.org/10.5802/crgeos.186.

DeNiro, M.J., Hastorf, C.A., 1985. Alteration of and ratios of plant matter during the initial stages of diagenesis: Studies utilizing archaeological specimens from Peru. Geochim. Cosmochim. Acta 49, 97–115. https://doi.org/10.1016/0016-7037(85)90194-2.

Espitalie, J., Deroo, G., Marquis, F., 1985. La pyrolyse Rock-Eval et ses applications. Deuxième Partie. Rev. Inst. Fr. Pét. 40, 755–784. https://doi.org/10.2516/ogst:1985045.

Espitalié, J., Laporte, J.L., Madec, M., Marquis, F., Leplat, P., Paulet, J., Boutefeu, A., 1977. Méthode rapide de caractérisation des roches mètres, de leur potentiel pétrolier et de leur degré d'évolution. Rev. Inst. Fr. Pét. 32, 23–42. https://doi.org/10.2516/ogst:1977002.

Everall, N.J., Lumsdon, J., Christopher, D.J., 1991. The effect of laser-induced heating upon the vibrational raman spectra of graphites and carbon fibres. Carbon 29, 133–137. https://doi.org/10.1016/0008-6223(91)90064-P.

Ferralis, N., Matys, E.D., Knoll, A.H., Hallmann, C., Summons, R.E., 2016. Rapid, direct and non-destructive assessment of fossil organic matter via microRaman spectroscopy. Carbon 108, 440–449. https://doi.org/10.1016/j.carbon.2016.07.039.

Ferrio, J.P., Alonso, N., López, J.B., Araus, J.L., Voltas, J., 2006. Carbon isotope composition of fossil charcoal reveals aridity changes in the NW Mediterranean Basin: carbon isotopes in charcoal and palaeoclimate. Glob. Chang. Biol. 12, 1253–1266. https://doi.org/10.1111/j.1365-2486.2006.01170.x.

Fidel, R.B., Laird, D.A., Spokas, K.A., 2018. Sorption of ammonium and nitrate to biochars is electrostatic and pH-dependent. Sci. Rep. 8, 17627. https://doi.org/10.1038/s41598-018-35534-w.

Fiorentino, G., Ferrio, J.P., Bogaard, A., Araus, J.L., Riehl, S., 2015. Stable isotopes in archaeobotanical research. Veget Hist. Archaeobot. 24, 215–227. https://doi.org/10.1007/s00334-014-0492-9.

Guo, Y., Bustin, R.M., 1998. Micro-FTIR spectroscopy of liptinite macerals in coal. Int. J. Coal Geol. 36, 259–275. https://doi.org/10.1016/S0166-5162(97)00044-X.

Hagemann, N., Joseph, S., Schmidt, H.-P., Kammann, C.I., Harter, J., Borch, T., Young, R. B., Varga, K., Taherymoosavi, S., Elliott, K.W., McKenna, A., Albu, M., Mayrhofer, C., Obst, M., Conte, P., Dieguez-Alonso, A., Orsetti, S., Subdiaga, E., Behrens, S., Kappler, A., 2017. Organic coating on biochar explains its nutrient retention and stimulation of soil fertility. Nat. Commun. 8, 1089. https://doi.org/10.1038/s41467-017-01123-0.

Hall, G., Woodborne, S., Scholes, M., 2008. Stable carbon isotope ratios from archaeological charcoal as palaeoenvironmental indicators. Chem. Geol. 247, 384–400. https://doi.org/10.1016/j.chemgeo.2007.11.001.

Hockaday, W.C., Grannas, A.M., Kim, S., Hatcher, P.G., 2006. Direct molecular evidence for the degradation and mobility of black carbon in soils from ultrahigh-resolution mass spectral analysis of dissolved organic matter from a fire-impacted forest soil. Org Geochem. 37, 501–510. https://doi.org/10.1016/j.orggeochem.2005.11.003.

Hossain, M.Z., Bahar, M.M., Sarkar, B., Donne, S.W., Ok, Y.S., Palansooriya, K.N., Kirkham, M.B., Chowdhury, S., Bolan, N., 2020. Biochar and its importance on nutrient dynamics in soil and plant. Biochar 2, 379–420. https://doi.org/10.1007/s42773-020-00065-z.

Khan, N., Clark, I., Bolan, N., Meier, S., Saint, C.P., Sánchez-Monedero, M.A., Shea, S., Lehmann, J., Qiu, R., 2017. Development of a buried bag technique to study biochars incorporated in a compost or composting medium. J. Soils Sediments 17, 656–664. https://doi.org/10.1007/s11368-016-1359-8.

Kleber, M., Lehmann, J., 2019. Humic substances extracted by alkali are invalid proxies for the dynamics and functions of organic matter in terrestrial and aquatic ecosystems. J. Environ. Qual. 48, 207–216. https://doi.org/10.2134/jeq2019.01.0036.

Lambrecht, G., Rodríguez de Vera, C., Jambrina-Enríquez, M., Crevecoeur, I., Gonzalez-Urquijo, J., Lazuen, T., Monnier, G., Pajović, G., Tostevin, G., Mallol, C., 2021. Characterisation of charred organic matter in micromorphological thin sections by means of Raman spectroscopy. Archaeol. Anthropol. Sci. 13, 13. https://doi.org/10.1007/s12520-020-01263-3.

Marguerie, D., Hunot, J.-Y., 2007. Charcoal analysis and dendrology: data from archaeological sites in north-western France. J. Archaeol. Sci. 34, 1417–1433. https://doi.org/10.1016/j.jas.2006.10.032.

Masi, A., Sadori, L., Baneschi, I., Siani, A.M., Zanchetta, G., 2013. Stable isotope analysis of archaeological oak charcoal from eastern Anatolia as a marker of mid-Holocene climate change: Climate change from Δ 13 C of current and mid-Holocene oak wood. Plant Biol. 15, 83–92. https://doi.org/10.1111/j.1438-8677.2012.00669.x.

Mouraux, C., Delarue, F., Bardin, J., Nguyen Tu, T.T., Bellot-Gurlet, L., Paris, C., Coubray, S., Dufraisse, A., 2022. Assessing the carbonisation temperatures recorded by ancient charcoals for δ13C-based palaeoclimate reconstruction. Sci Rep 12, 14662. 10.1038/s41598-022-17836-2.

Naseem, H., Ahsan, M., Shahid, M.A., Khan, N., 2018. Exopolysaccharides producing rhizobacteria and their role in plant growth and drought tolerance. J. Basic Microbiol. 58, 1009–1022. https://doi.org/10.1002/jobm.201800309.

Romero-Sarmiento, M.-F., Pillot, D., Letort, G., Lamoureux-Var, V., Beaumont, V., Huc, A.-Y., Garcia, B., 2016. New rock-eval method for characterization of unconventional shale resource systems. Oil Gas Sci. Technol. – Rev. IFP Energies Nouvelles 71, 37. https://doi.org/10.2516/ogst/2015007.

Rouzaud, J.-N., Deldicque, D., Charon, É., Pageot, J., 2015. Carbons at the heart of questions on energy and environment: A nanostructural approach. C. R. Geosci. 347, 124–133. https://doi.org/10.1016/j.crte.2015.04.004.

Salavert, A., Dufraisse, A., 2014. Understanding the impact of socio-economic activities on archaeological charcoal assemblages in temperate areas: A comparative analysis of firewood management in two Neolithic societies in Western Europe (Belgium, France). J. Anthropol. Archaeol. 35, 153–163. https://doi.org/10.1016/j.jaa.2014.05.002.

Schmidt, M.W.I., Noack, A.G., 2000. Black carbon in soils and sediments: Analysis, distribution, implications, and current challenges. Global Biogeochem. Cycles 14, 777–793. https://doi.org/10.1029/1999GB001208.

Sigmund, G., Santín, C., Pignitter, M., Tepe, N., Doerr, S.H., Hofmann, T., 2021. Environmentally persistent free radicals are ubiquitous in wildfire charcoals and remain stable for years. Commun. Earth Environ. 2, 68. https://doi.org/10.1038/s43247-021-00138-2.

Solomon, D., Lehmann, J., Kinyangi, J., Liang, B., Schäfer, T., 2005. Carbon K-edge NEXAFS and FTIR-ATR spectroscopic investigation of organic carbon speciation in soils. Soil Sci. Soc. Am. J. 69, 107–119. https://doi.org/10.2136/sssaj2005.0107dup.

Sykes, R., Snowdon, L.R., 2002. Guidelines for assessing the petroleum potential of coaly source rocks using Rock-Eval pyrolysis. Org Geochem. 33, 1441–1455. https://doi.org/10.1016/S0146-6380(02)00183-3.

Turney, C.S.M., Wheeler, D., Chivas, A.R., 2006. Carbon isotope fractionation in wood during carbonization. Geochim. Cosmochim. Acta 70, 960–964. https://doi.org/10.1016/j.gca.2005.10.031.

Vaiglova, P., Snoeck, C., Nitsch, E., Bogaard, A., Lee-Thorp, J., 2014. Impact of contamination and pre-treatment on stable carbon and nitrogen isotopic composition of charred plant remains. Rapid Commun. Mass Spectrom. 28, 2497–2510. https://doi.org/10.1002/rcm.7044.

Vandenbroucke, M., Behar, F., Espitalie, J., 1988. Characterization of sedimentary organic matter by preparative pyrolysis: comparison with Rock Eval pyrolysis and pyrolysis-gas chromatography techniques. Energy Fuels 2, 252–258. https://doi.org/10.1021/ef00009a004.

Weng, Z., Van Zwieten, L., Tavakkoli, E., Rose, M.T., Singh, B.P., Joseph, S., Macdonald, L.M., Kimber, S., Morris, S., Rose, T.J., Archanjo, B.S., Tang, C., Franks, A.E., Diao, H., Schweizer, S., Tobin, M.J., Klein, A.R., Vongsvivut, J., Chang, S.L.Y., Kopittke, P.M., Cowie, A., 2022. Microspectroscopic visualization of how biochar lifts the soil organic carbon ceiling. Nat. Commun. 13, 5177. https://doi.org/10.1038/s41467-022-32819-7.

Wiedner, K., Fischer, D., Walther, S., Criscuoli, I., Favilli, F., Nelle, O., Glaser, B., 2015. Acceleration of biochar surface oxidation during composting? J. Agric. Food Chem. 63, 3830–3837. https://doi.org/10.1021/acs.jafc.5b00846.

Yan, H., Liu, C., Yu, W., Zhu, X., Chen, B., 2023. The aggregate distribution of Pseudomonas aeruginosa on biochar facilitates quorum sensing and biofilm formation. Sci. Total Environ. 856, 159034 https://doi.org/10.1016/j.scitotenv.2022.159034.

Zeba, N., Berry, T.D., Panke-Buisse, K., Whitman, T., 2022. Effects of physical, chemical, and biological ageing on the mineralization of pine wood biochar by a Streptomyces isolate. PLoS One 17, e0265663. https://doi.org/10.1371/journal.pone.0265663.